



ORIGINAL ARTICLE

Hyper-branched multifunctional carbon nanotubes carrier for targeted liver cancer therapy



Yadong Zhou^a, Kandasamy Vinothini^{b,*}, Fafu Dou^a, Yan Jing^a,
Anil A. Chuturgoon^c, Thilona Arumugam^c, Mariappan Rajan^b

^a Department of Gastrointestinal Surgery, 3201 Hospital, Hanzhong 723000, China

^b Biomaterials in Medicinal Chemistry Laboratory, Department of Natural Products Chemistry, School of Chemistry, Madurai Kamaraj University, Madurai 625021, Tamil Nadu, India

^c Discipline of Medical Biochemistry and Chemical Pathology, Faculty of Health Sciences, University of KwaZulu-Natal, Durban 4041, South Africa

Received 15 September 2021; accepted 13 December 2021

Available online 17 December 2021

KEYWORDS

Carbon nanotubes;
Doxorubicin;
HepG2 liver cancer cell line;
Multifunctional nanocarrier system

Abstract The systemic toxicity of anticancer drugs regularly restricts the use of conventional chemotherapy to treat cancer. In this study, the limitations overcome by profitably fabricating a multifunctional nanocarrier system to carry the anticancer drug into the specific location of the cancer cells. The polyethylene glycol (PEG) was functionalized in the carboxylated multiwalled carbon nanotubes (MWCNT-COOH) through an esterification reaction (MWCNT-PEG). The targeting ligand of folic acid (FA) was covalently bonded with hyperbranched poly-L-lysine (HBPLL) using adipic acid (AA) as a cross-linking agent. Doxorubicin (DOX), an anticancer drug, was effectively loaded on MWCNT-PEG-AA-HBPLL-FA carrier loading, and *in-vitro* drug release was investigated by UV-Vis spectrophotometer. The chemical functionalization, morphological properties, crystalline nature, surface charge, and thermal stability of the synthesized materials were studied by FT-IR, FE-SEM, HR-TEM, DLS, and TGA techniques. *In-vitro* cytotoxicity and anticancer properties of DOX-loaded nanocarrier were studied in human liver cancer (HepG2) cells and human embryonic kidney (HEK293) cells. The activities of caspases (caspase -3, -8 & -9) were analyzed using luminometry. The intrinsic apoptosis pathway proteins (Bcl-2 & BAX) were determined by western blot and RT-PCR analysis. The synthesized DOX-loaded nanocarriers exhibited increased cytotoxicity and apoptosis in liver HepG2 cells. The results suggest that the DOX-loaded

* Corresponding author.

E-mail address: vinothini81094@gmail.com (K. Vinothini).

Peer review under responsibility of King Saud University.



nanocarrier possesses strong anticancer properties and could be an applicable and potential drug carrier for liver cancer chemotherapy.

© 2021 The Author(s). Published by Elsevier B.V. on behalf of King Saud University. This is an open access article under the CC BY-NC-ND license (<http://creativecommons.org/licenses/by-nc-nd/4.0/>).

1. Introduction

Chemotherapy is widely used as one of the main strategies for treating cancers, and the method of chemotherapy commonly involves the binding of anticancer drugs to the DNA of target tumor cells to inhibit cell division, DNA replication, and cell deaths (Morabito et al., 2006; Peng et al., 2020). However, chemo-resistance is an important source of treatment defeat, and these medicines induce adverse side effects due to their low targeting efficiency. The problem of drug resistance can be resolved by targeted drug delivery. An advantage of targeted drug delivery is that the drugs are released only in the tumor, thus minimizing toxicity to normal and healthy cells (Trindade et al., 2000; Fraguas-Sanchez et al., 2020).

Various carbon materials' distinctive physical and chemical properties make their use in biomedical applications, optoelectronics, energy storage devices, etc. (Novoselov et al., 2004; Ghitescu et al., 2018; Mandal et al., 2016). Carbon nanotubes (CNTs) are very attractive cylindrical carbon atoms composed of a multi-layer of graphene sheets. Research focusing on CNTs has increased as they hold promise in biomedical research, like drug delivery vehicles, careful cell spoliation factors, biosensors, cellular growth substrates, and prosthetic implants (Muthu et al., 2013; Heister et al., 2013; Taghdisi et al., 2011). One of the critical roles of CNTs in biomedical applications is they can comfortably penetrate the cells. They can improve perform as an ideal delivery vehicle to deliver various drugs and dyes (Kostarelos et al., 2009). Further, the drug-loaded nanocarrier has an appropriate size range at 10–200 nm to quickly accumulate into the tumor places called enhanced permeation and retention effect (EPR) (Mohamed et al., 2021).

The polyethylene glycol (PEG) increases the biodegradability of carbon-based materials; the PEG is an FDA-approved biocompatible polymer, which has good aqueous solubility, non-toxicity, good biocompatibility, and non-immunogenicity (Kaldybekov et al., 2019). Amongst these, the major challenge during cancer treatment is to synthesize carriers that possess safety and efficiency. Hyperbranched polymeric drug delivery systems are increasing the safety of carrier systems to enhance their efficacy. Adeli et al., 2013 reported cisplatin loaded citric acid-glycerol polyester nanocarrier exhibits good biocompatible carrier to deliver drug molecules on affected sites (Cheng et al., 2011; Adeli et al., 2013). However, these researchers failed to deliver the anticancer drug to the target site in diseased cells. Since folic acid is an ideal targeting ligand, it is convenient for targeting cancer cell membranes and attractive nanoparticle endocytosis via the folate receptor. The folate receptor is a 38 kDa glycosyl-phosphatidylinositol conjugated glycoprotein, which is overexpressed on cancer cell surfaces such as breast, ovarian, uterus, lung, liver, and colon cancer cell membranes (Vinothini et al., 2019; Pradeepkumar et al., 2018). Doxorubicin, an anthracycline class of chemotherapeutic drug, is widely used

as an anticancer drug; it inhibits the DNA synthesis needed for proliferating cells (Wu et al., 2014).

A hyperbranched MWCNT nanocarrier system was prepared with the loading doxorubicin drug to treat cancer disease. The amine functionalities of polylysine are used for the covalent coupled hyperbranched MWCNT-PEG synthesis. The PEG has been chosen as it is a biodegradable polymer to improve the dispersing nature of the MWCNT. Further, we introduced poly-L-lysine to create an electrostatic interaction between negatively charged cancer cell membranes. The targeting ligand is used to improve the specific delivery of DOX drug into the cancer cells. From the investigation, the results demonstrate that the targeting ligand of FA covalently conjugated with hyperbranched polymer helps in intracellular drug delivery of DOX to FA receptor overexpressed cancer cell membranes to inhibit the cancer cells.

2. Materials and methods

2.1. Materials

MWCNT was obtained from SRL Chemicals Ltd, Mumbai, India. Polyethylene glycol (PEG, Mw = 6000), Thionyl chloride (SOCl₂), Adipic acid (AA), L-lysine hydrochloride, and Potassium hydroxide (KOH) were purchased from Sigma Aldrich Co., Ltd, Mumbai, India. Tetrahydrofuran (THF), *N, N*-dimethylformamide (DMF), Triethylamine (TEA), Methanol (MeOH), and sulfuric acid were purchased from Merck Co., Ltd, Mumbai, India. Folic acid (FA) and Doxorubicin (DOX) were received from Sigma Aldrich, Mumbai, India. The other reagents were analytical grade, and all reagents were used without any further purification.

2.2. Synthesis of MWCNT-PEG polymer from MWCNT-COCl

The carboxylated multiwalled carbon nanotubes (MWCNT-COOH) (100 mg) were dispersed in 25 mL of DMF solvent and subjected to probe ultra-sonication (SONICS Vibra-Cell) for 30 min for 130 W with 5 sec on 2 sec off and the frequency of 20 kHz. Then, the homogeneous carboxylated MWCNT solution was transferred into 250 mL round bottom flask, further mixed with 20 mL of thionyl chloride and addition of 5 mL *N, N*-dimethylformamide (DMF) as a catalyst and heated to 75 °C under magnetic stirring for 24 h. The solution was then washed with anhydrous tetrahydrofuran (THF) to remove the unreacted SOCl₂ and DMF solvent. The obtained compound was dried at 60 °C under a hot air oven overnight to get MWCNT-COCl. Further, the samples were used for further characterizations and reactions. The MWCNT-COCl (50 mg) was added into 200 mg containing PEG polymer in 50 mL of (v/v = 3/1) benzene/water mixture, and the mixture was stirred under 80 °C at 40 h. After the reaction was completed, the black precipitate of MWCNT-PEG polymer was centrifuged at 3000 rpm for 15 min, further washed with dis-

tilled water. Finally, the brownish-black substance was dried in a hot air oven for 24 h (Wei et al., 2018). Additionally, the product was collected and stored.

2.3. Synthesis of MWCNT-PEG-AA

The MWCNT-PEG-AA was synthesized by the condensation reaction with MWNT-PEG and adipic acid (AA), and the reaction was followed by a previously reported procedure with slight modifications (Ahmadi Azghandi et al., 2017). Typically, 50 mg of MWNT-PEG was dispersed in 50 mL of distilled water. Then 50 mg of adipic acid was added to the system, further 5 mL of concentrated H₂SO₄ were added slowly and heated to 120 °C for 12 h with continuous stirring on the magnetic stirrer. Further, the product was washed away with distilled water and dried at 60 °C in a hot air oven for 24 h. Then, the final compounds were collected and used for further experimental sections.

2.4. Synthesis of hyperbranched poly-L-lysine (HBPLL)

Hyperbranched poly-L-lysine (HBPLL) was prepared as per the procedure previously reported by Guangyue et al. (Guangyue et al., 2016). Briefly, L-lysine hydrochloride (5.479 g, 30.0 mmol) and potassium hydroxide (1.52 g, 27.05 mmol) were thoroughly mixed with mortar until a consistent mixture was formed. The substance was moved into a 500 mL three-necked RB flask and added 25 mL of paraffin oil,; the compound was kept at 150 °C for 48 h under N₂ atmosphere during the whole polymerization process remove the water. Then, the substance was cooled at room temperature (27 °C). Afterward, eliminating paraffin oil, several times washed with petroleum ether; further, the excess of petroleum ether was evaporated. The attained brownish-yellow solid compound was then fully dissolved in methanol solution, the obtained by products of KCl were removed by filtration using Whatman filter paper 2.5 μm size (G.No-42). Further, the THF solvent was added to obtain the yellow-brown precipitate, and the residue was recovered and dissolved in distilled water. Then, the precipitate solution was adjusted pH value to 5.0. Finally, the compound was dialyzed using a dialysis bag (MWCO-12000) against double distilled water and then lyophilized (SSIPL-LYF/065/071216) under -40 °C.

2.5. FA and MWCNT-PEG-AA tagged hyperbranched HBPLL synthesis

The MWCNT-PEG-AA and FA functionalized HBPLL were prepared through previous reported one and slight changes (Wen et al., 2013). In brief, HBPLL (50 mg) dissolved in DMSO (5 mL) with an equal ratio of MWCNT-PEG-AA (10 mg) and FA (10 mg) (1:1) was separately dissolved in DMSO (5 mL) solution carboxylic acid groups were activated by EDC.HCl (10.0 mg) and NHS (10.0 mg) was magnetically stirred for 2 h. Afterward, the activated carboxylic groups were mixed dropwise into the HBPLL solution. The reaction was continued with stirring for 3 days to obtain HBPLL conjugated MWCNT-PEG-AA-FA nanocarrier. The obtained material was dialyzed for 48 h against distilled water. The final products were lyophilized (SSIPL-LYF/065/071216) under -40 °C.

2.6. Synthesis of DOX-loaded multifunctional HBPLL-functionalized MWCNT-PEG-AA-HBPLL-FA.

The DOX-loaded nanocarrier was prepared through the solvent evaporation method (Pradeepkumar et al., 2017). The anticancer drug of doxorubicin (3 mg/mL) solution was dissolved in a 5 mL ethanol solution and mixed with HBPLL-functionalized MWCNT-PEG-AA-HBPLL-FA solution (30 mg/mL) and stirred for 24 h at room temperature (27 °C). The final DOX/MWCNT-PEG-AA-HBPLL-FA was collected and washed by ultracentrifugation (5,000 rpm, 30 min) to remove the unbound DOX molecule. The drug encapsulation and loading content of DOX were determined UV-Vis spectrophotometrically at λ_{max} value of 494 nm of DOX.

2.7. Determination of drug encapsulation and drug loading capacity

Drug encapsulation and loading capacity were studied using the DOX/MWCNT-PEG-AA-HBPLL-FA carrier, and then free DOX was then measured after the supernatant solution was centrifuged. The loading capacity of DOX was determined by UV-Vis spectrophotometer 494 nm. Thus, the percentage (%) of drug encapsulation efficiency and loading capacity was calculated using the below formulas:

$$EE(\%) = \frac{\text{Total amount of drug} - \text{Free amount of drug}}{\text{Total amount of drug}} \times 100$$

$$LC(\%) = \frac{\text{Total amount of drug} - \text{Free amount of drug}}{\text{Weight of the dried nanocarrier}} \times 100$$

2.8. In-vitro drug release study

The *in-vitro* drug release properties of the DOX/MWCNT-PEG-AA-HBPLL-FA carrier were evaluated by the dialysis method. Briefly, 10 mg of DOX/MWCNT-PEG-AA-HBPLL-FA carrier was placed into a dialysis bag with a molecular weight cut-off (MWD) of 10,000 kDa. Furthermore, the dialysis bag was submerged in 50.0 mL of PBS at different pHs like 2.8, 5.5, 6.8 & 7.4 at 27 °C with gentle stirring on a magnetically stirred for 150 rpm. At an every 3 h time intervals, 2 mL of the sample suspension was withdrawn from the PBS release medium and replaced with an equal volume of fresh PBS suspension. Finally, the DOX release medium was determined by the UV-vis spectrometer (Shimadzu-1600, Japan) at a λ_{max} value of 494 nm.

2.9. Biological studies

2.9.1. Cell culture

The HepG2 human liver carcinoma cells and HEK239 human embryonic kidney cells were cultured at 37 °C, 5% CO₂ in complete culture media (CCM), (Eagles Minimum Essential media, supplemented with 10% fetal calf serum, 1% L-glutamine, and 1% penicillin-streptomycin-fungizone) until 90% confluent. Once confluent, the cells were collected by trypsinization and used for further studies.

2.9.2. Cell viability

The WST-1 assay was used to study the cell viability of the synthesized sample. In brief, both cell lines were seeded with 96-well plates at 1×10^4 /well and incubated overnight at 37 °C with 5% CO₂. After that, the cells were incubated for 24 h with various concentrations of MWCNT-PEG-AA-HBPLL-FA and DOX/MWCNT-PEG-AA-HBPLL-FA carrier in (0–150 µg/mL). The WST-1 solution (50 µL, 2 mg/mL) was added to each well and incubated for 4 h; after the supernatant was discarded, and 100 µL of DMSO was added to each and incubated for 1 h at 37 °C. Finally, the absorbance intensity was determined using a spectrophotometer (Bio-Tek µQuant) at a wavelength of 450 nm. The viable cell percentage was measured, and a dose-response curve was generated from which the IC₅₀ value was extrapolated.

2.9.3. Mitochondrial membrane potential ($\rho\psi m$)

In brief, 1×10^4 HepG2 human liver carcinoma cells and HEK239 human embryonic kidney cells were seed in six-well plates and resuspended overnight. After that, the cells were treated with MWCNT-PEG-AA-HBPLL-FA and DOX/MWCNT-PEG-AA-HBPLL-FA carrier for 24 h; further, the cells were washed with PBS and stained with JC-1 stain (5 mg/mL) for 20 mins at 37 °C in the dark condition. The Mitochondrial Membrane Potential ($\rho\psi m$) was measured under the Nikon Eclipse Ti fluorescence microscope (Nikon Instruments Inc.).

2.9.4. Caspase assay

The Caspase Glo® 8, 9, and 3 assay kits (Promega, Madison, USA) were used to detect the caspase activity. The cells were seeded in 96-well plates at 1×10^4 /well alongside 20 mL of caspase Glo® reagent were added and incubated under dark conditions for 30 min at ambient room temperature. The luminescence was captured and quantified using a Modulus™ microplate luminometer (Turner Biosystems, Sunnyvale, USA). The data were shown as mean relative light units (RLU).

2.9.5. Microscopy analysis

The Hoechst 33342 stain (Cat # H1399, Thermo Fisher Scientific, Waltham, MA, USA) was used to distinguish the nuclear damage of cells. The cells were cultured with a 3.4 cm² diameter culture dish over sterile coverslips until 80% confluence, further treated with different concentrations of MWCNT-PEG-AA-HBPLL-FA and DOX/MWCNT-PEG-AA-HBPLL-FA nanocarrier. After 24 h incubation, the cell was stained with 5 µg/mL of Hoechst 33342 for 15 min, washed with PBS, and mounted over the glass slide. Nucleus changes were captured using fluorescence microscopy.

2.9.6. Western blotting

The human HepG2 liver carcinoma cells were treated with MWCNT-PEG-AA-HBPLL-FA and DOX/MWCNT-PEG-AA-HBPLL-FA carrier used to induce apoptosis for 24 h. After treatment, cells were lysed with RIPA buffer, and the protein concentration of cell lysates was measured using the DC Protein Assay Reagent (Bio-Rad, Hercules, CA, USA). Proteins were separated using gel electrophoresis (2 h at 100 V) and transferred into nitrocellulose membrane (wet

transfer; 2 h at 80 V). Primary antibodies (Bcl-2: mouse monoclonal antibody, Cat# 13–8800; BAX: mouse monoclonal antibody, Cat# 336400; GAPDH: mouse monoclonal antibody, Cat# MA5-15738) and secondary antibody HRP conjugated (Goat anti-mouse HRP, Cat# A90-234P) from Thermo Fisher Scientific, (Waltham, MA, USA) were used. The target proteins were visualized using an ECL detection kit (Millipore, Burlington, MA, USA). Chemi luminescence signals were captured using Chemi-Doc Imaging Systems. Band density was quantitated using Image J Software (National Institutes of Health, Bethesda, MD, USA) (see Fig. 1).

2.9.7. Real-time PCR

Quantitative gene expression was evaluated by SYBR green master mix (Cat # A25741, Thermo Fisher Scientific, Waltham, MA, USA). RNeasy Mini kit (Cat # 74134, Qiagen, NJ, USA) was used to isolate RNA from cultured cells according to the manufacturer's instructions. About 1–2 µg of RNA was used to produce cDNA using the iScript cDNA synthesis kit based on the manufacturer's protocol (Cat#1708890, Bio-Rad, Hercules, CA, USA). The PCR amplification was performed in 40 cycles using the following program: 95 °C for 10 min (hold), 95 °C for 15 s, and 60 °C for 1 min. GAPDH is used as a housekeeping control. Data were analyzed using the $2^{-\Delta\Delta Ct}$ method. The primer sequences used as follows:

Gene	Forward primer	Reverse primer
Bcl-2	5'-GCTGGACA TTGGA CTTCCTC-3	5'-GCTGGA CATTG GACTTCCTC-3'
BAX	5'-GCTGGACATTG GACTTCCTC-3'	5'-ACCACTGT GACCTGCTCCA-3'
GAPDH	5'-ACCCAGAA GACTGTGGATGG-3'	5'-TTCTAGACGG CAGGTCAGGT-3

3. Results and discussion

3.1. FT-IR and XRD analysis

In order to distinguish the structural changes of MWCNT-COOH, MWCNT-PEG, MWCNT-PEG-AA, MWCNT-PEG-AA-HBPLL-FA, and DOX/MWCNT-PEG-AA-HBPLL-FA carriers are investigated using FT-IR spectroscopy (Fig. 2A). FT-IR spectrum of carboxylate MWCNT is represented in Fig. 2A(a). A broad, strong peak at 3309 cm⁻¹ indicates the -OH group of the carboxylic MWCNT, and the stretching vibrations at 1740 cm⁻¹, 1641 cm⁻¹, and 1023 cm⁻¹ represent the functional groups of C=O, C=C, and C-O, respectively. The peak at 2925 cm⁻¹ corresponds to the presence of a C-H stretching bond (Mahinpour et al., 2018). After functionalization with PEG on the carboxylic acid group of MWCNT surface, the higher shift of carbonyl peaks at 1740 cm⁻¹ to 1743 cm⁻¹ due to the formation of ester linkage as presented in Fig. 2A(b) (Vasheghani Farahani et al., 2016). Fig. 2A(c) displays the FT-IR spectrum of adipic acid-functionalized MWCNT-PEG. A new strong attained absorption peak at the range of

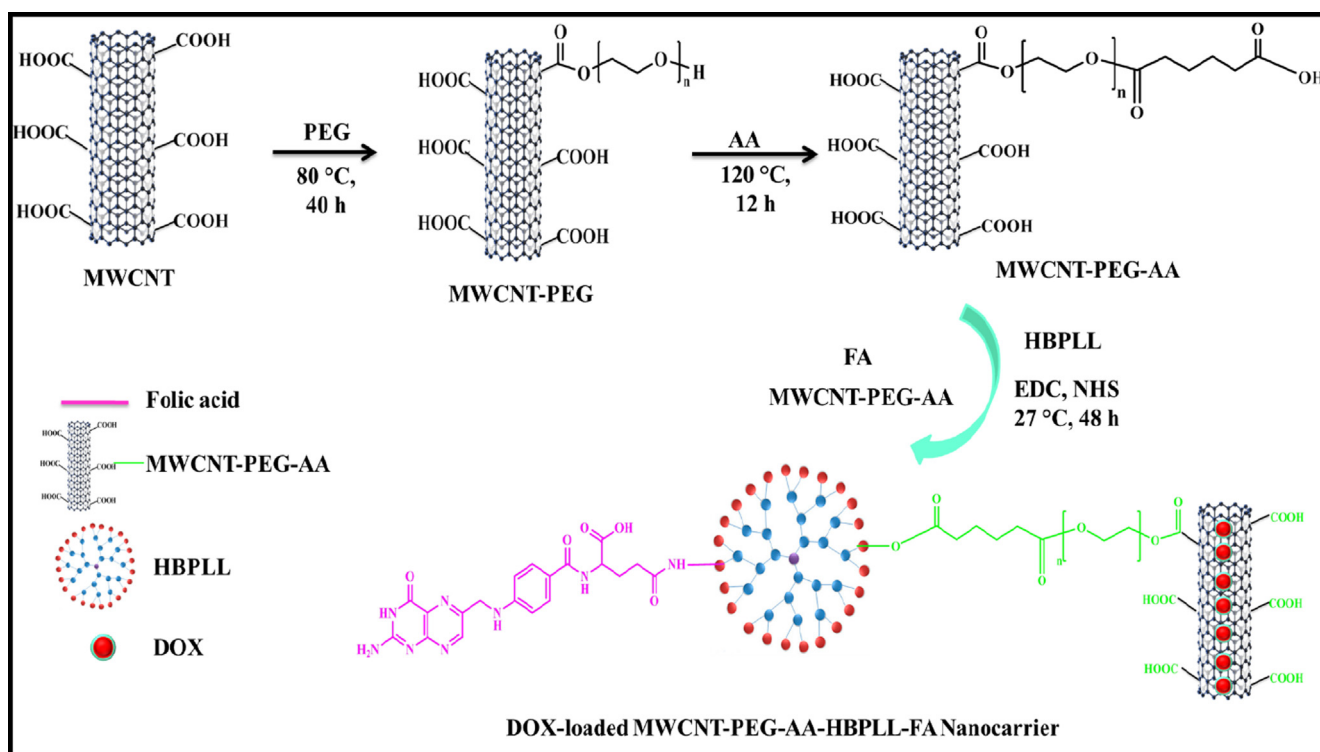


Fig. 1 Overall schematic illustration of DOX/MWCNT-PEG-AA-HBPLL-FA carrier synthesis.

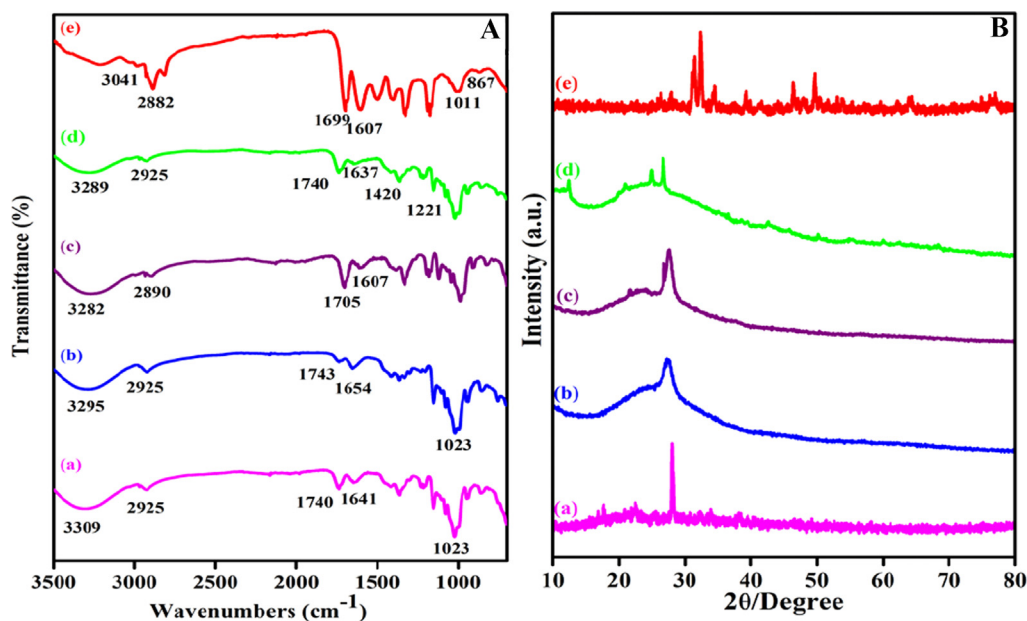


Fig. 2 (A) FTIR spectra of (a) MWCNT-COOH, (b) MWCNT-PEG, (c) MWCNT-PEG-AA, (d) MWCNT-PEG-AA-HBPLL-FA carrier and (e) DOX/MWCNT-PEG-AA-HBPLL-FA carrier and (B) XRD pattern of (a) MWCNT-COOH, (b) MWCNT-PEG, (c) MWCNT-PEG-AA, (d) MWCNT-PEG-AA-HBPLL-FA carrier and (e) DOX/MWCNT-PEG-AA-HBPLL-FA carrier.

1705 cm^{-1} is observed from another ester bond that indicates adipic acid was successfully conjugated with MWCNT-PEG (Ahmadi Azghandi et al., 2017). The HBPLL polymer combined with MWCNT-PEG-AA and FA to appear in two new amide bonds at 1637 cm^{-1} and 1420 cm^{-1} , which ascribed to the amide linkages of $-\text{C}=\text{O}-\text{NH}-$ stretching vibration and

N-H bending vibration (Nasrollahi et al., 2016) consistently (Fig. 2A(d)). It demonstrates the successful covalent conjugation of FA and MWCNT-PEG-AA into HBPLL polymer. From FT-IR spectra of Fig. 2A(e) signify the DOX/MWCNT-PEG-AA-HBPLL-FA carrier in the spectrum of the carbonyl peaks at 1641 cm^{-1} and 1023 cm^{-1} were shifted

into higher and lower positions at 1699 cm^{-1} and 1011 cm^{-1} , which can be introduced by the formation of hydrogen bonds and π - π stacking interaction between DOX and MWCNT carrier. A new peak appeared at 867 cm^{-1} and 3042 cm^{-1} due to the presence of out-of-plane N-H vibration and N-H stretching vibration of DOX molecule (Dong et al., 2013). We also well correlated with early Adeli et al., 2013 proposed poly amidoamine poly (ethylene glycol)-poly amidoamine (PAMAM-PEG-PAMAM) nanotubes shows that liposomes like structures which effectively encapsulate and deliver the drug molecules on affected areas (Adeli et al., 2013). It reveals that the prepared carrier proves the successful loading of DOX on the MWCNT surface through physical interactions.

The crystalline phase differentiation of MWCNT based carrier and DOX loaded MWCNT carrier systems was examined by XRD spectroscopy. The XRD pattern of Fig. 2B(a), denotes the MWCNT-COOH; the typical characteristic diffraction peak at 27° appeared by 002 plane exhibit the sharp peak corresponds due to the crystalline nature of the MWCNT-COOH. This peak also correlated with Egbosiuba et al., (2020), previously reported multiwalled carbon nanotubes are also crystalline in nature (Egbosiuba et al., 2020). After functionalization with the hydrophilic polymer of PEG, the MWCNT Sharp peak intensity was diminished, which indicate in Fig. 2B(b). Further, AA functionalized MWCNT-PEG also introduces the same broad-like peak at 26° as given in Fig. 2B(c). The appeared peaks at 12° , 20° , and 24° also confirmed the functionalization of FA and MWCNT-PEG-AA on HBPLL polymer (Fig. 2Bd), which also correlated with previously Chen et al., reported folic acid functionalized aminated multiwalled carbon nanotubes using targeted drug delivery system (Kayat et al., 2015). Moreover, DOX/MWCNT-PEG-AA-HBPLL-FA carrier represents the peaks such as 27° , 31° , 32° , and 44° was observed and confirms the poly amorphous natured drug-loaded carrier, which is more helpful due to the easy distribution of drug molecules on tumors sites.

3.2. Morphological analysis

The surface morphology of MWCNT-COOH, MWCNT-PEG, MWCNT-PEG-AA-HBPLL-FA, and DOX/MWCNT-PEG-AA-HBPLL-FA was characterized by using SEM and HR-TEM analysis as given in Fig. 3. The MWCNT-COOH clearly shows a tubular-like structure (Fig. 3a). After PEG reaction in MWCNT shows a cluster form of PEG attached MWCNT edges, as illustrated in Fig. 3(b). In addition, the modification of HBPLL polymer in MWCNT-PEG-AA and FA morphology was detected and given in Fig. 3(c), which displays that curled-like tubular structure also indicates the successful conjugation of successful conjugation FA and MWCNT-PEG-AA and the average scale bar range of MWCNT-PEG-AA-HBPLL-FA is $1\text{ }\mu\text{m}$ from SEM analysis. The DOX molecule was loaded on the MWCNT-PEG-HBPLL-AA-FA surface to obtain a sporadic coil-like structure. The yellow marked arrow indicates the evidence of DOX loading on the carrier through physical interactions between the DOX and MWCNT-PEG-AA-HBPLL-FA carrier (Fig. 3d).

HR-TEM study used analysis of the intrinsic surface morphology of as-prepared CNT-based carrier and drug-loaded carrier systems; it was well correlated with SEM analysis. HR-TEM images of (Fig. 3e) prove a tubular-like structure of MWCNT-COOH. Fig. 3f indicates the presence of hydrophilic PEG on grafted with MWCNT surface edges. Moreover, the presence of PEG on the MWCNT surface appeared in entangled MWCNT morphology, which determines the improved dispersion properties during the carbon-based drug carrier system. Further, the MWCNT-PEG-AA and FA were connected with the polymeric material of HBPLL to form an enlarged polymeric network-like structure in Fig. 3(g). Also, the drug molecule bounded on the MWCNT-PEG-AA-HBPLL-FA carrier shows an interconnected network-like structure represented in Fig. 2(h). Finally, the tubular-like

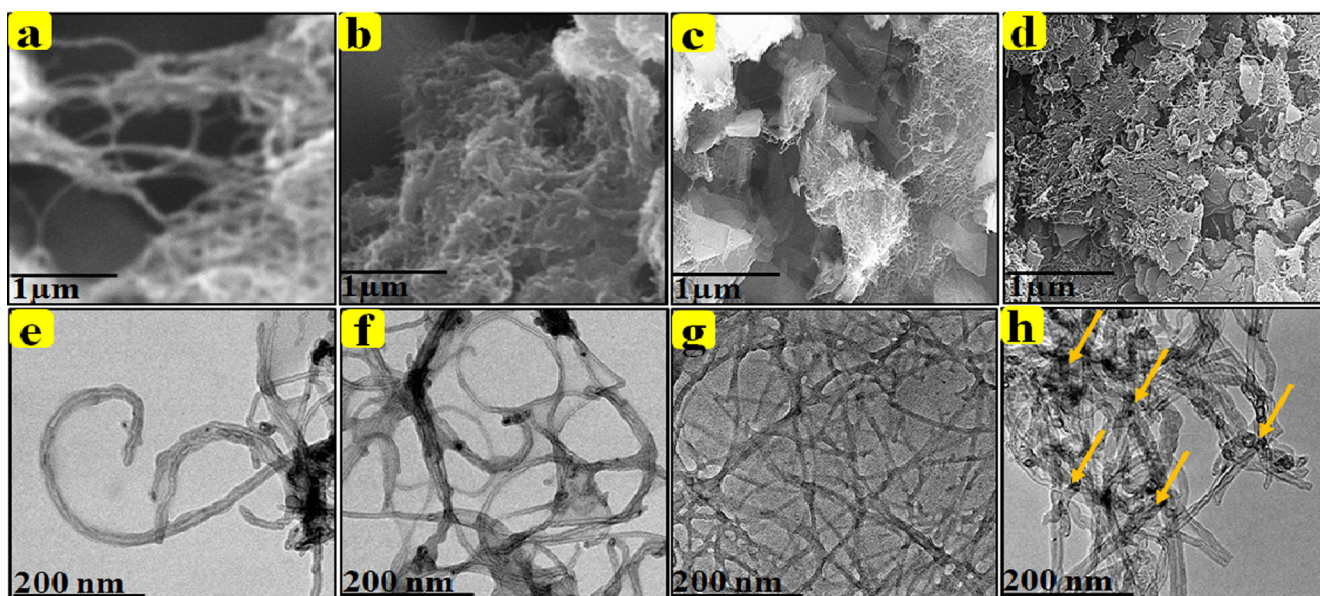


Fig. 3 SEM and HR-TEM images: MWCNT-COOH, MWCNT-PEG, MWCNT-PEG-AA-HBPLL-FA, and DOX/MWCNT-PEG-AA-HBPLL-AA-FA carrier.

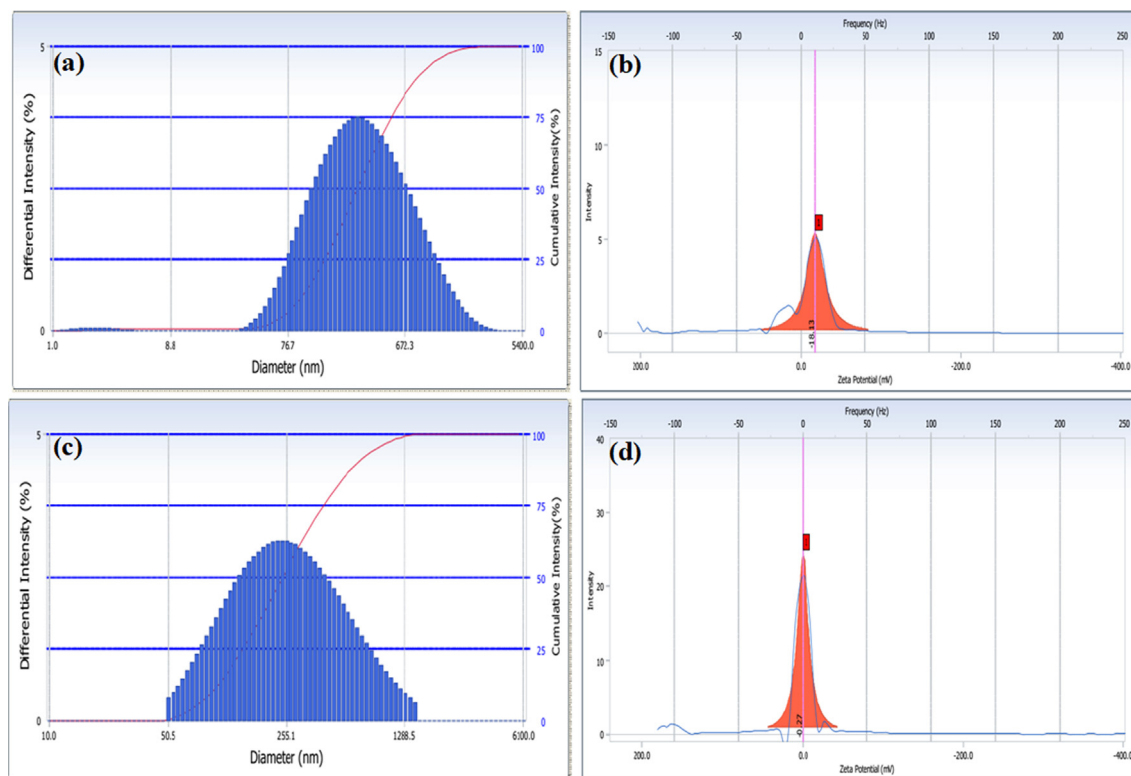


Fig. 4 Particle size and zeta potential analysis of MWCNT-PEG-AA-HBPLL-FA (a&b) DOX/MWCNT-PEG-AA-HBPLL-FA carrier (c&d).

morphology of the carbon-based carrier system created the ideal platform for the high loading and releasing nature of cancer drug delivery systems.

3.3. Particle size distribution and zeta potential measurements

The average particle size of MWCNT-PEG-AA-HBPLL-FA was 365 nm, whereas the diameter range of DOX/MWCNT-PEG-AA-HBPLL-FA was 392 nm denoted in Fig. 4. The MWCNT-PEG-AA-HBPLL-FA carrier, after that the loading of DOX molecule on MWCNT surface the particle size was enlarged. The PDI for MWCNT-PEG-AA-HBPLL-FA before and after loading with DOX was 0.168 and 0.183 correspondingly. It finds out the non-symmetric nature of MWCNT. Besides, the obtained PI values were < 0.4 , demonstrating the dependability of the reported size values with some homogeneity (Raza et al., 2016). The zeta potential value of DOX with and without a carrier is -18.13 mV and -0.27 mV (Fig. 4b,d). The DOX/MWCNT-PEG-AA-HBPLL-FA carrier surface charge was decreased, which designates the loading of DOX on the MWCNT surface. It also indicates that the prepared MWCNT based carrier is stable in a neutral medium. The stability of the carrier plays a vital role in newly synthesized drug cargo systems.

Moreover, the zeta potential results strongly indicate the DOX/MWCNT-PEG-AA-HBPLL-FA carrier stability and use for potential drug carrier applications (Guo et al. 2018). Further, the highly negative charge of the nanocarrier was greatly interactive with the positive cell membrane. These results are also related to the previously Vinothini et al. developed a magnetic nanocarrier having a stable and suitable drug

cargo system on cancer sites due to the promising biological interaction of carrier and cancer cell walls (Vinothini et al., 2020).

3.4. Thermal analysis (TGA)

Thermal stability and decomposition nature of (a) MWCNT-COOH, (b) MWCNT-PEG, (c) MWCNT-PEG-AA-HBPLL-FA, and (d) DOX/MWCNT-PEG-AA-HBPLL-FA carrier were examined through thermal gravimetric analysis, and the results are established in Fig. 5. As can be seen, From in Fig. 5 (a), is TGA spectrum of MWCNT-COOH represent the decomposition of $-COOH$ group at 81% weight loss indicates to elimination of H_2O & CO_2 on MWCNTs-COOH surface (Bruno et al., 2017). After functionalized with PEG exhibits two distinct stages of weight losses of 14%, and 74% was observed at 200–600 °C, which describes the loss of oxygen-containing functional (H_2O , CO_2 , & CO) groups grafted on MWCNT surface (Meihua Tan et al., 2020). Our TGA analysis also well correlated with previously Maria et al., 2020 proposed MWCNT-COOH and PEG functionalized MWCNT-PEG exhibits high thermal stability (Maria et al., 2020). The thermal decomposition of the MWCNT-PEG-AA-HBPLL-FA carrier displays three stages of decomposition (Fig. 5c). Significantly, the weight loss of MWCNT-PEG-AA-HBPLL-FA indicates that amino groups functionalized material was more stable, and they could involve in some thermal reaction at a temperature more than 400 °C. The first step is due to the weight loss of the moisture and H_2O groups at 90–100 °C, while the second step introduces the decomposition of polymer combined ester and CO_2 molecules up to 110–

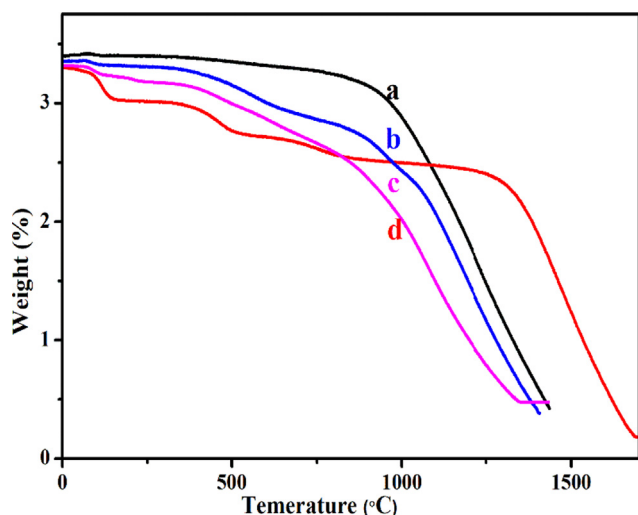


Fig. 5 TGA thermal stability of (a) MWCNT-COOH, (b) MWCNT-PEG, (c) MWCNT-PEG-AA-HBPLL-FA, and (d) DOX/MWCNT-PEG-AA-HBPLL-FA carrier.

300 °C, in the third step indicated the deterioration of amide linkages at degradation temperature range at 300–700 °C, as compared to DOX-loaded carrier, the DOX molecules interacted with MWCNT surface through physical interactions, when the temperature was also increased up (Meihua Tan et al., 2020) to 700 °C, the DOX molecules were totally dissociated on the MWCNT wall surface and the weight ratio at 88%, which indicated the thermal stability of MWCNT-PEG-AA-HBPLL-FA carrier. Finally, our results concluded that the functional groups are effectively grafted with the MWCNT surface.

3.5. Encapsulation efficiency and *in-vitro* drug release studies

The drug encapsulation efficiency and loading capacity are the two major parameters for designing and developing effective drug delivery carrier systems (Meysam et al., 2021). The DOX/MWCNT-PEG-AA-HBPLL-FA carrier in drug-releasing rates exists in Fig. 6. The DOX was encapsulated with MWCNT-PEG-AA-HBPLL-FA carrier surface through physical interactions like electrostatic and π - π stacking interactions. The UV-Vis spectrum of the DOX/MWCNT-PEG-AA-HBPLL-FA carrier shows the DOX region absorbance peak at 494 nm. The DOX encapsulation efficiency was obtained at 62.5%, and the loading capacity of DOX is 25.4%, separately. These results indicate a high amount of the drugs was successfully encapsulated on the MWCNT-PEG-AA-HBPLL-FA carrier. Finally, high encapsulating and loading efficiency bounded carriers will help and improve the *in-vitro* drug delivery application.

The drug release rates of DOX from the carrier were explored at three different physiological pHs (2.8, 5.5, 6.8 & 7.4) at room temperature, and the results are assumed in Fig. 6. The UV-Visible spectroscopy analysis recorded a sustained DOX drug release nature of the DOX/MWCNT-PEG-AA-HBPLL-FA carrier. At 24 h investigation, a maximum of 92.0 % of DOX release rate was observed in acidic

2.8 pH. The physically interacted DOX molecule was easily cleavable in acidic conditions. Meanwhile, DOX molecules are readily soluble in the acidic medium because the $-\text{NH}_2$ group of DOX was quickly protonated (Zhang et al., 2017) on the acidic medium from MWCNT based materials are efficient drug delivery carrier system for biomedical applications. Fig. 6 (e) shows the cumulative drug release pattern of MWCNT-PEG-AA-HBPLL-FA carrier, the release rate of DOX at pH-5.5 is 84 %, pH-6.8 is 32 %, and pH -7.4 is 28% drug release with the 24 h intervals. Finally, the acidic condition was the most suitable environment for the release of drugs in tumor cells.

3.6. *In-vitro* cytotoxicity studies

The *in-vitro* cell viability of MWCNT-PEG-AA-HBPLL-FA and DOX/MWCNT-PEG-AA-HBPLL FA carriers were determined using human liver cancer (HepG2) cell line and human embryonic kidney (HEK239) cell lines subsequently. Both cell lines were treated with varying concentrations of (0–150 $\mu\text{g}/\text{mL}$) as prepared compounds, and the cytotoxic results are given in Fig. 7. The cytotoxic effect was increased with increasing concentrations of MWCNT-PEG-AA-HBPLL-FA and DOX/MWCNT-PEG-AA-HBPLL-FA carriers. After 24 h incubation periods, we have observed clear cell death in both cell lines. Fig. 7(a&b) shows that the MWCNT-PEG-AA-HBPLL-FA and DOX/MWCNT-PEG-AA-HBPLL-FA nanocarriers treated HEK239 cell line exhibits less cytotoxic effects, which proved that our prepared nanocarrier has good biocompatible nature in the normal cell line. Further, in Fig. 7(c&d), MWCNT-PEG-AA-HBPLL-FA treated HepG2 cell line shows minimum cell death. After that, the DOX/MWCNT-PEG-AA-HBPLL-FA treated liver cancer HepG2 cell line manifested a higher amount of cytotoxic effect because the anticancer drug of DOX has effectively inhibited topoisomerase I permitting DNA damages in a cancer cell line, over a 24 h incubation period. Finally, the IC_{50} values for both normal and cancer cell line treated MWCNT-PEG-AA-HBPLL-FA and DOX/MWCNT-PEG-AA-HBPLL-FA non-carrier were observed at 170.4, 86.94 $\mu\text{g}/\text{mL}$ and 210.1, 425.1 $\mu\text{g}/\text{mL}$, respectively.

3.7. JC-1 mitochondrial depolarization

We measured mitochondrial depolarization of the cells as an indicator of apoptosis being induced by MWCNT-PEG-AA-HBPLL-FA (DU) and DOX/MWCNT-PEG-AA-HBPLL-FA (DL) carriers in both HepG2 and HEK239 cells using the IC_{50} concentrations. In Fig. 8, the DOX loaded MWCNT-PEG-AA-HBPLL-FA shows that membrane depolarization increased. The membrane depolarization increases were reduced cell proliferation due to increased oxidative stress and mitochondrial pathway induced apoptosis.

3.8. Caspase activity assay

The intracellular caspase activation is one of the main tools or the apoptosis cell death pathway, which leads to the cleavage and inactivation of many cellular proteins. In the present

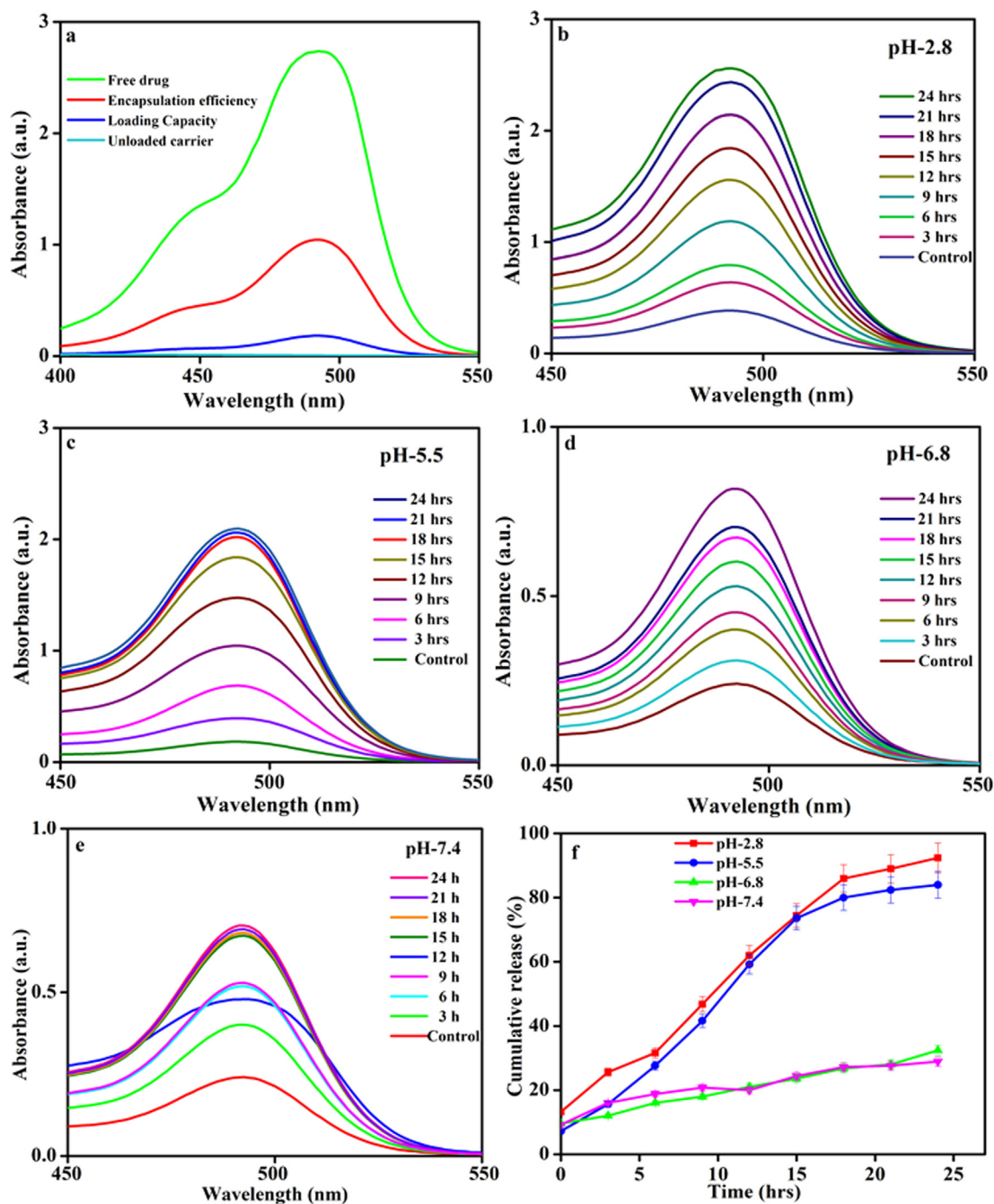


Fig. 6 (a) Encapsulation efficiency and (b, c, d, & e) *In-vitro* drug release profiles of various physiological conditions like pH-2.8, pH-5.5, pH-6.8 & pH-7.4 and (e) Cumulative drug-releasing profile of DOX/MWCNT-PEG-AA-HBPLL-FA carrier.

study, the caspase activations of -8 , -9 , & -3 were investigated at 24 h incubation of MWCNT-PEG-AA-HBPLL-FA and DOX/MWCNT-PEG-AA-HBPLL-FA carrier. The results demonstrate that MWCNT-PEG-AA-HBPLL-FA carrier treated HepG2 cell exhibits significant upregulation caspase activity of -8 & -9 , and downregulation caspase activity of -3 . Moreover, the DOX/MWCNT-PEG-AA-HBPLL-FA carrier treated HepG2 cell introduce decreasing the whole caspase -8 , -9 , and -3 activity compared with control as shown

in Fig. 9. In these results, our fabricated DOX/MWCNT-PEG-AA-HBPLL-FA carrier significantly induced cells *via* intrinsic apoptotic signaling pathway.

3.9. Hoechst staining

Cellular nuclear damage was analyzed using fluorescence microscopy. The bright blue fluorescent Hoechst stain is a cell internalized nucleic acid dye (Syed Abdul Rahman et al.,

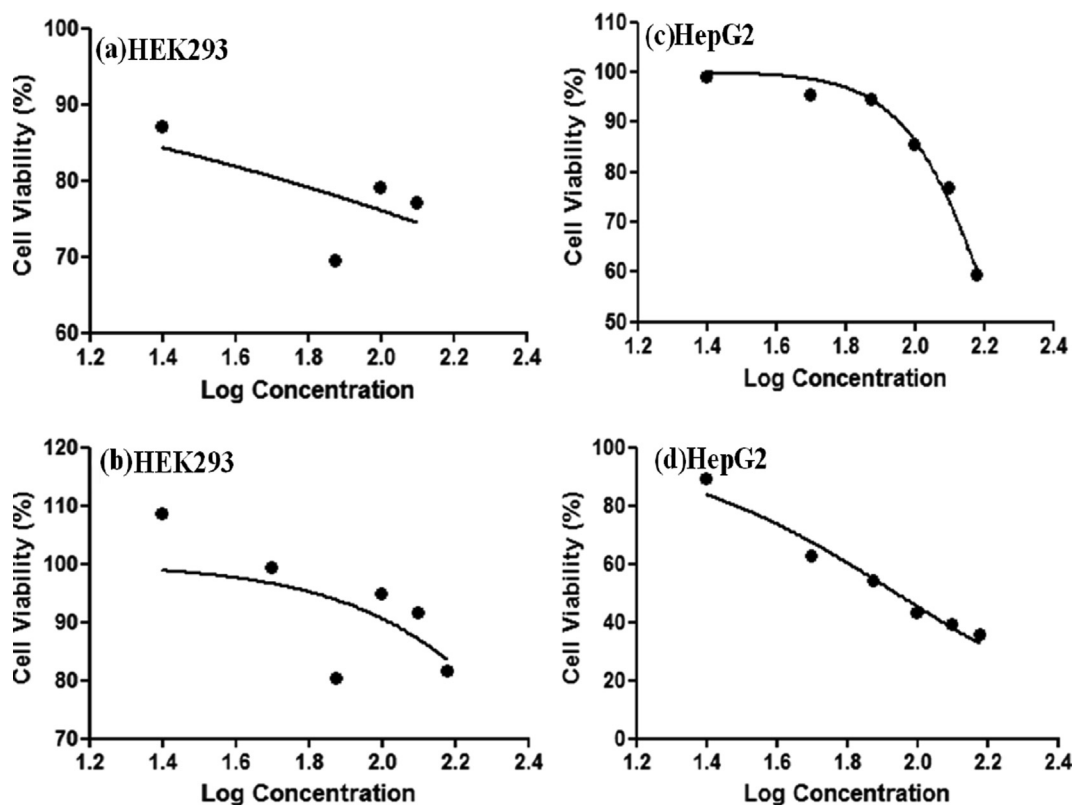


Fig. 7 *In-vitro* cell viability of HEK293 (a&b) and HepG2 (c&d) cell line incubated with varying concentrations of MWCNT-PEG-AA-HBPLL-FA and DOX/MWCNT-PEG-AA-HBPLL-FA carrier.

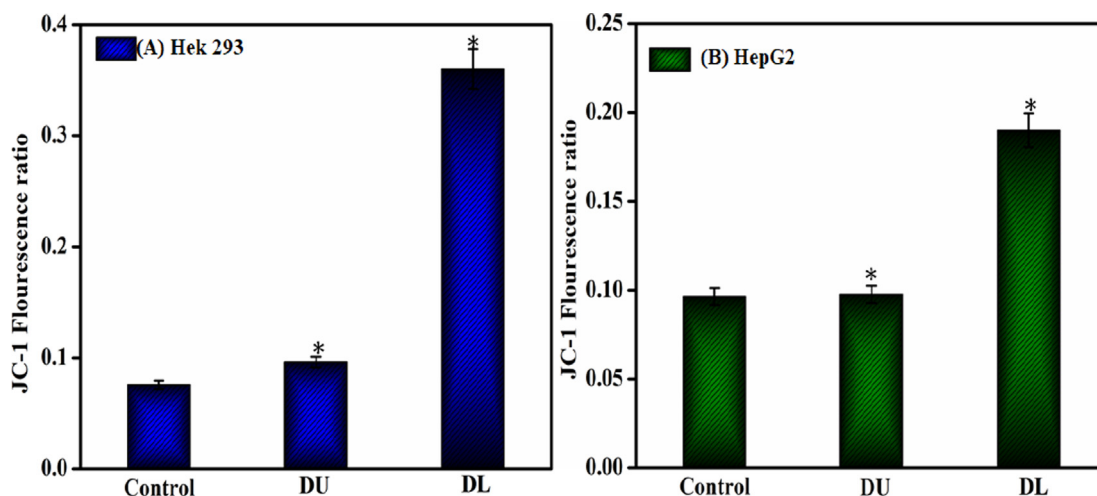


Fig. 8 Mitochondrial depolarization effect of MWCNT-PEG-AA-HBPLL-FA (DU) and DOX/MWCNT-PEG-AA-HBPLL-FA (DL) carrier treated with IC_{50} concentrations.

2013), which is widely used to analyze the nucleus damage and fragmentation of apoptotic cells. Fig. 10 shows the nuclear damage in HepG2 cells after 24 h treatment of DOX with/without nanocarrier-loaded compounds. The control cell appeared to be intact oval shapes and bright blue fluorescent dye. In contrast, the DOX/MWCNT-PEG-AA-HBPLL-FA carrier treated cells showed less fluorescent intensity, unclear cell shapes, and a damaged nucleus. These results suggested

that the DOX/MWCNT-PEG-AA-HBPLL-FA carrier is highly efficient to inducing cell death in HepG2 cells.

3.10. Apoptosis analysis

The pro-apoptotic and anti-apoptotic proteins are generally involved in cell proliferation and cell death. In this study, the two apoptosis-related proteins, Bcl-2 and BAX, were analyzed

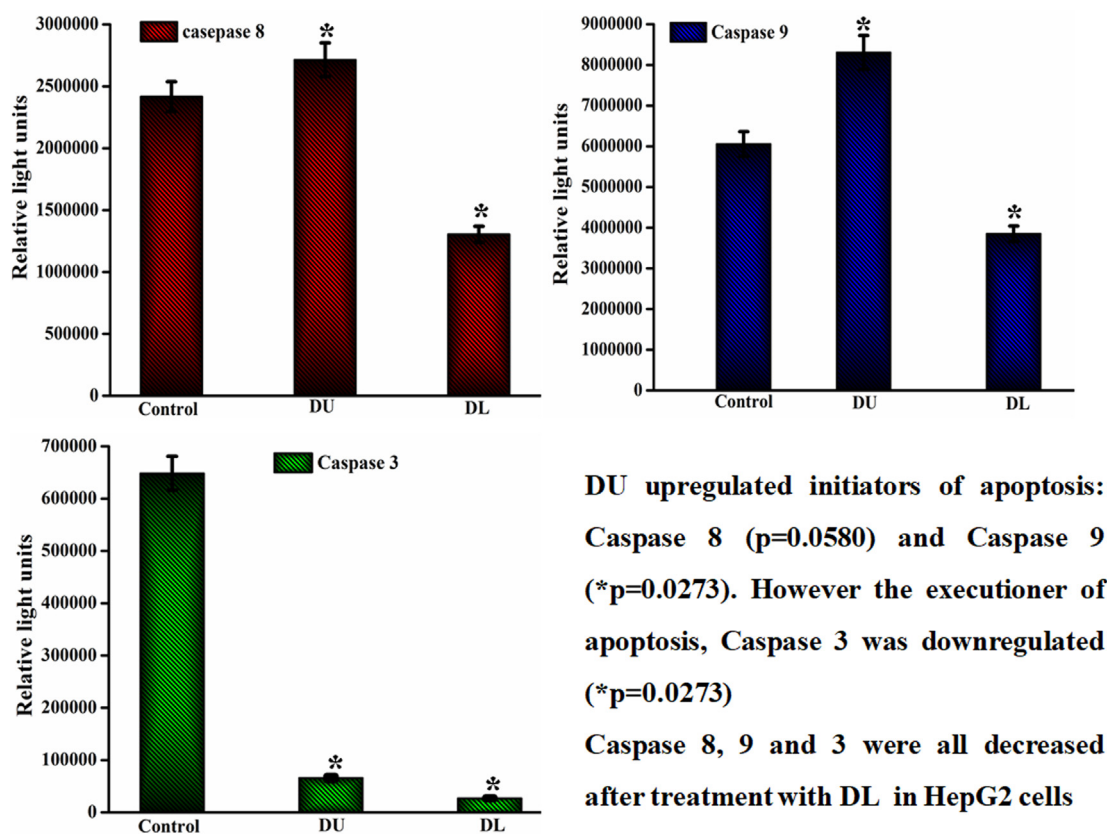


Fig. 9 Caspase -8, -9 & -3 activities of MWCNT-PEG-AA-HBPLL-FA (DU) and DOX/MWCNT-PEG-AA-HBPLL-FA (DL) carriers treated with IC_{50} concentrations.

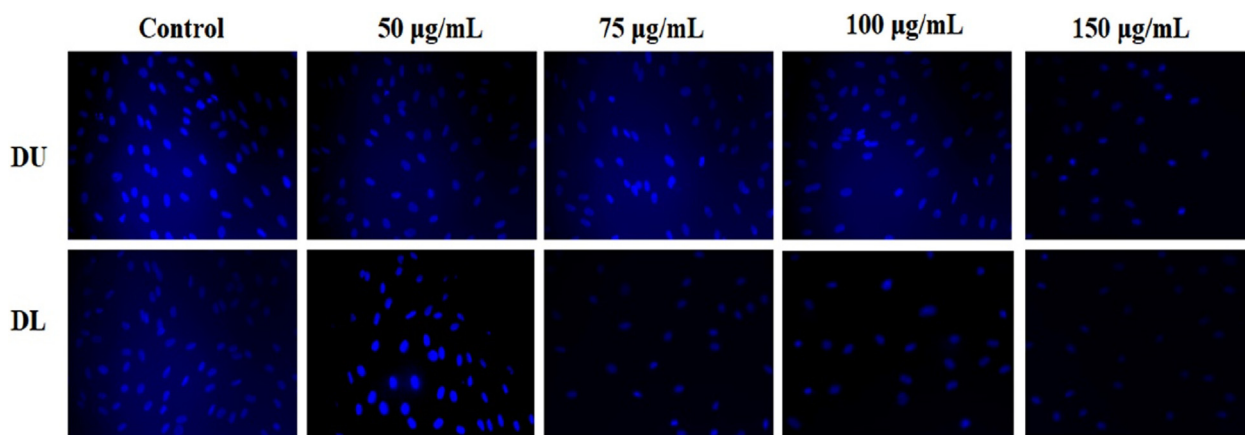


Fig. 10 The fluorescent images of HepG2 cells incubated with various concentrations of MWCNT-PEG-AA-HBPLL-FA and DOX/MWCNT-PEG-AA-HBPLL-FA nanocarrier stained with Hoechst stain.

using western blotting. Fig. 11(a&b) shows the western blot images of Bcl-2 and BAX in DOX/MWCNT-PEG-AA-HBPLL-FA treated and control groups of HepG2 cells. DOX is widely used as a potent anticancer agent as it is a potent inducer of apoptosis. The anti-apoptotic protein Bcl-2 mainly inhibits the mitochondrial pathway (Vivek et al. 2014). BAX is a pro-apoptotic protein that promotes apoptosis in cells, although it was present in inactivating states in many cancers. The treatment with DOX/MWCNT-PEG-AA-HBPLL-FA nanocarrier upregulated the protein and gene

expression of BAX and down-regulated the expression of Bcl-2. These results strongly support the observations that DOX/MWCNT-PEG-AA-HBPLL-FA is a potent inducer of cell death in cancer cells by increased apoptosis.

4. Conclusion

In this study, the synthesized MWCNT nanoparticles were successfully loaded with DOX. These nanoparticles showed efficient drug loading capacity, targeted and pH-dependent

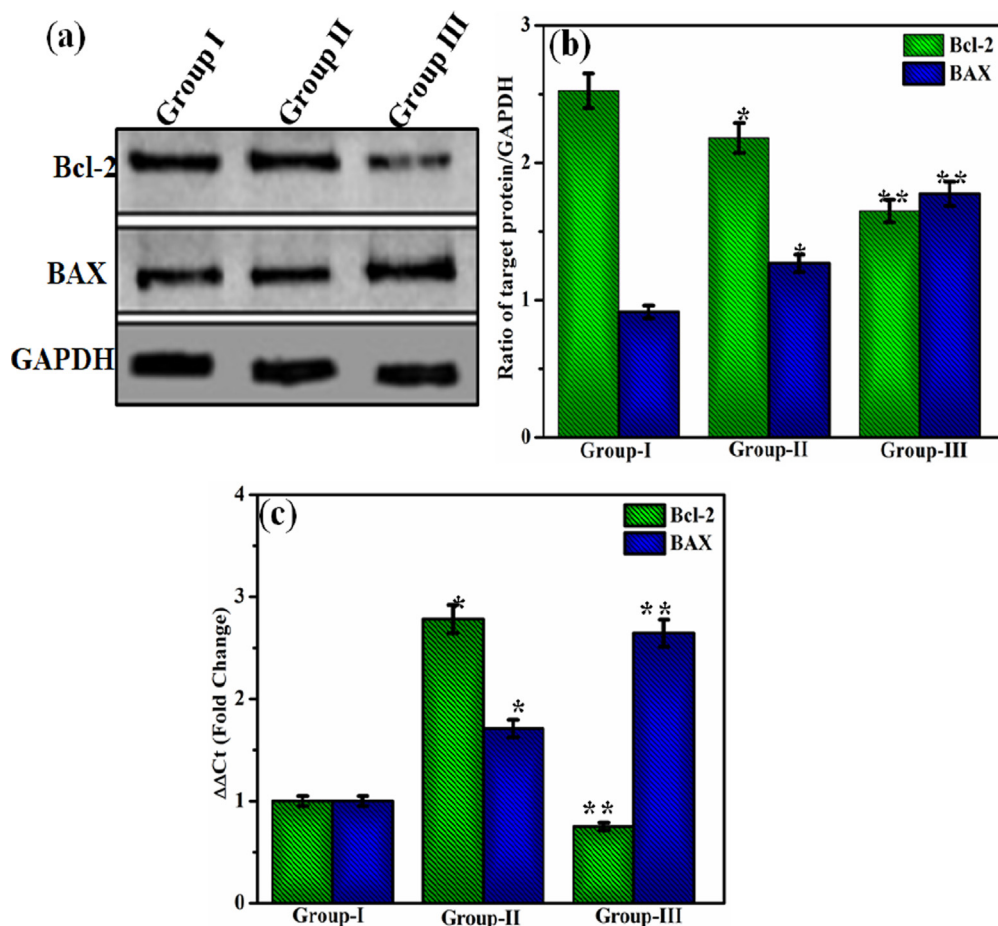


Fig. 11 (a) Representative blot of Bcl-2 and BAX levels in HepG2 cells, (b) Ratio of Bcl-2 and BAX to GAPDH. Error bars represent SEM from three replicates (* $P < 0.05$) (c) mRNA expression of Bcl-2 and BAX in HepG2 cells. Group I- Control; Group II- DU; Group III- DL. Error bars represent SEM from three replicates (* $p < 0.05$).

drug release in a cancer cell line; this observation is important as it can overcome the conventional chemotherapy treatments limitations such as easy binding of prepared nanoparticles with cancer cell receptor, which leads to quick entering of the receptor-mediated endocytosis and delivered the drug on affected areas. A high amount of drug release rate was observed at acidic pH conditions on intracellular endosomes environments. *In vitro* models were used to show that the nanoparticles were highly cytotoxic to HepG2 cells but minimally cytotoxic to HEK293 cells. Further MWCNT nanoparticles increased nuclear fragmentation in HepG2 cells, leading to upregulating both the protein and gene expression of BAX and downregulating of Bcl-2 expression. Finally, caspase activities of (-8, -9 & -3) reveal that the activation of the intrinsic apoptotic pathway was favored in HepG2 cells. Overall, the DOX/MWCNT-PEG-AA-HBPLL-FA nanocarrier system provides a potential approach for a reliable targeted drug delivery system for cancer chemotherapy.

CRediT authorship contribution statement

Yadong Zhou: Conceptualization, Data curation, Formal analysis, Investigation, Software, Writing – original draft, Writing – review & editing. **Kandasamy Vinothini:** Conceptualization,

Data curation, Formal analysis, Funding acquisition, Investigation, Methodology, Project administration, Resources, Software, Supervision, Validation, Visualization, Writing – original draft, Writing – review & editing. **Fafu Dou:** Data curation, Formal analysis, Investigation, Software, Writing – original draft, Writing – review & editing. **Yan Jing:** Data curation, Formal analysis, Investigation, Software, Writing – original draft, Writing – review & editing. **Anil A. Chuturgoon:** Data curation, Formal analysis, Investigation, Methodology, Project administration, Resources, Software, Supervision, Validation, Visualization, Writing – original draft, Writing – review & editing. **Thilona Arumugam:** Data curation, Formal analysis, Investigation, Software, Writing – original draft, Writing – review & editing. **Mariappan Rajan:** Conceptualization, Data curation, Formal analysis, Funding acquisition, Investigation, Methodology, Project administration, Resources, Software, Supervision, Validation, Visualization, Writing – original draft, Writing – review & editing.

Declaration of Competing Interest

The authors declare that they have no known competing financial interests or personal relationships that could have appeared to influence the work reported in this paper.

Acknowledgement

M. Rajan appreciates the financial support under the plan of the Science and Engineering Research Board (Ref: YSS/2015/001532; New Delhi, India) and also acknowledges the PURSE program for the purchase of SEM, FT-IR, and UPE programs for the purchase of HR-TEM. K. Vinothini thanks to the Council of Scientific and Industrial Research (CSIR), New Delhi for Senior Research Fellowship (Ref.no.0 9/201(0428)/2020-EMR-I).

Appendix A. Supplementary material

Supplementary data to this article can be found online at <https://doi.org/10.1016/j.arabjc.2021.103649>.

References

- Adeli, M., Rasoulia, B., Saadatmehr, F., Zabihi, F., 2013a. Hyper-branched poly (citric acid) and its application as anticancer drug delivery system. *J. Appl. Polym. Sci.* 129, 3665–3671.
- Adeli, M., Beyranvand, S., Kabiri, R., 2013b. Preparation of hybrid nanomaterials by supramolecular interactions between dendritic polymers and carbon nanotubes. *Polym. Chem.* 4, 669.
- Ahmadi Azghandi, M.H., Vasheghani Farahani, B., Dehghani, N., 2017. Encapsulation of methotrexate and cyclophosphamide in interpolymer complexes formed between poly acrylic acid and poly ethylene glycol on multiwalled carbon nanotubes as drug delivery systems. *Mater. Sci. Eng., C* 79, 841–847.
- Bruno, E., Olivier, B., Andrea, M., Roberto, L., Alexandru, V., Jean, F.G., 2017. Electroactive polymer/carbon nanotube hybrid materials for energy storage synthesized via a “grafting to” approach. *RSC Adv.* 7, 17301.
- Cheng, J.P., Mezziani, M.J., Sun, Y.P., Cheng, S.H., 2011. Poly (ethylene glycol)-conjugated multiwalled carbon nanotubes as an efficient drug carrier for overcoming multidrug resistance. *Toxicol. Appl. Pharmacol.* 250, 184.
- Dong, Q., Yi, S., Peng, Z., Zhao, C., 2013. The preparation and the invitro pharmacodynamics study of the intracapsular sustained-release preparations for the prevention of posterior capsule opacification. *Asian J. Pharm. Sci.* 8, 252–260.
- Egboosiuba, T.C., Abdulkareem, A.S., Kovo, A.S., Afolabi, E.A., Tijani, J.O., Roos, W.D., 2020. Enhanced adsorption of As(V) and Mn (VII) from industrial wastewater using multiwalled carbon nanotubes and carboxylated multiwalled carbon nanotubes. *Chemosphere* 254, 126780.
- Fraguas-Sanchez, A.I., Fernandez-Carballido, A., Delie, F., Cohen, M., Martin-Sabroso, C., Mezzanzanica, D., Figini, M., Satta, A., Torres-Suarez, A.I., 2020. Enhancing ovarian cancer conventional chemotherapy through the combination with cannabidiol loaded microparticles. *Eur. J. Pharm. Biopharm.* 154, 246–258.
- Ghitescu, R.E., Maria Popa, A., Schipanski, A., Hirsch, C., Yazgan, G., Popa, V.I., Rossi, R.M., Maniura-Weber, K., Fortunato, G., 2018. Catechin loaded PLGA submicron-sized fibers reduce levels of reactive oxygen species induced by MWCNT in vitro. *Eur. J. Pharm. Biopharm.* 122, 78–86.
- Guangyue, Z., Min, L., Kunchi, Z., Shanni, H., Jingjin, D., Yi, C., Bin, J., Liqiang, L., Renjun, P., 2016. Functional hyperbranched polylysine as potential contrast agent probes for magnetic resonance imaging. *Biomacromolecules* 17, 2302–2308.
- Guo, B., Liao, C., Liu, X., Yi, J., 2018. Preliminary study on conjugation of formononetin with multiwalled carbon nanotubes for inducing apoptosis via ROS production in hela cells. *Drug Design Dev. Ther.* 12, 2815–2826.
- Heister, E., Brunner, E.W., Dieckmann, G.R., Jurewicz, I., Dalton, A. B., 2013. Are carbon nanotubes a natural solution? *Appl. Biol. Med. ACS Appl. Mater. Interfaces* 5, 1870–1891.
- Kaldybekov, D.B., Filippov, S.K., Radulescu, A., Khutoryanskiy, V. V., 2019. Maleimide functionalised PLGA-PEG nanoparticles as mucoadhesive carriers for intravesical drug delivery. *Eur. J. Pharm. Biopharm.* 143, 24–34.
- Kayat, J., Mehra, N., Gajbhiye, V., Jain, N., 2015. Drug targeting to arthritic region via folic acid appended surface-engineered multi-walled carbon nanotubes. *J. Drug. Target.* 22, 318–327.
- Kostarelos, K., Bianco, A., Prato, M., 2009. Promises, facts and challenges for carbon nanotubes in imaging and therapeutics. *Nat. Nanotechnol.* 4, 627–633.
- Mahinpour, R., Moradi, L., Zahraei, Z., Pahlevanzadeh, N., 2018. New synthetic method for the synthesis of 1,4-dihydropyridine using aminated multiwalled carbon nanotubes as high efficient catalyst and investigation of their antimicrobial properties. *J. Saudi Chem. Soc.* 22, 876–885.
- Mandal, B., Das, D., Rameshbabu, A., Dhara, S., Pal, S., 2016. A biodegradable, biocompatible transdermal device derived from carboxymethyl cellulose and multiwalled carbon nanotubes for sustained release of diclofenac sodium. *RSC Adv.* 6, 19605–19611.
- Maria, N., Cristian, G., Elisa F., 2020. Proteomic exploration of soft and hard biocorona onto PEGylated multiwalled carbon nanotubes. *Int. Union Biochem. Mol. Biol. Inc.* 0, 1–11.
- Meihua Tan, J., Bullo, S., Fakurazi, S., Zobir Hussein, M., 2020. Preparation, characterisation and biological evaluation of biopolymer coated multi walled carbon nanotubes for sustained delivery of silibinin. *Scientific Reports* 10, 16941.
- Meyam, S., Mohammad, V., Asgari, M., 2021. Preparation of hyaluronic acid-decorated mixed nanomicelles for targeted delivery of hydrophobic drugs to CD44-overexpressing cancer cells. *Int. J. Pharm.* 592, 120052.
- Mohamed, M.E., Zakaria, A.B., Mohamed, I.A.D., Ahmed, K.E.S., Magy, M.A., Ayman, H., 2021. *In vivo* toxicity and antitumor activity of newly green synthesized reduced graphene oxide/silver nanocomposites. *Bioresour. Bioprocess.* 8, 44.
- Morabito, A., Longo, R., Gattuso, D., Carillio, G., Massaccesi, C., Mariani, L., Bonginelli, P., Amici, S., De Sio, L., Fanelli, M., Torino, F., Bonsignori, M., Gasparini, G., 2006. Trastuzumab in combination with gemcitabine and vinorelbine as second-line therapy for HER-2/neu overexpressing metastatic breast cancer. *Oncol. Rep.* 16, 393–398.
- Muthu, M.S., Abdulla, A., Pandey, B.L., 2013. Major toxicities of carbon nanotubes induced by reactive oxygen species: should we worry about the effects on the lungs, liver and normal cells? *Nanomedicine* 8, 863–866.
- Nasrollahi, F., Varshosaz, J., Ali Khodadadi, A., Lim, S., Najafabadi, A.J., 2016. Targeted delivery of docetaxel by use of transferrin/poly (allylamine hydrochloride)- functionalized graphene oxide nanocarrier. *ACS Appl. Mater. Interfaces.* 8, 13282–13293.
- Novoselov, K.S., Geim, A.K., Morozov, S.V., Jiang, D., Zhang, Y., Dubonos, S.V., Grigorieva, I.V., Firsov, A.A., 2004. Electric field effect in atomically thin carbon films. *Science* 306, 666–669.
- Peng, F., Li, R., Zhang, F., Qin, L., Ling, G., Zhang, P., 2020. Potential drug delivery nanosystems for improving tumor penetration. *Eur. J. Pharm. Biopharm.* 151, 220–238.
- Pradeepkumar, P., Govindaraj, D., Jeyaraj, M., Munusamy, M.A., Rajan, M., 2017. Assembling of multifunctional latex-based hybrid nanocarriers from *Calotropis gigantea* for sustained (doxorubicin) DOX releases. *Biomed. Pharmacother.* 87, 461–470.
- Pradeepkumar, P., Rajendran, N., Alarfaj, A.A., Munusamy, M.A., Rajan, M., 2018. Deep eutectic solvent-mediated FA-g-β-alanine-co-PCL drug carrier for sustainable and site-specific drug delivery. *ACS Appl. Bio Mater.* 1, 2094–2109.
- Raza, K., Kumar, D., Kiran, C., Kumar, M., Kumar Guru, S., Kumar, P., Arora, S., Sharma, G., Bhushan, S., Katare, O.P., 2016. Conjugation of docetaxel with multiwalled carbon nanotubes and

- codelivery with piperine: implications on pharmacokinetic profile and anticancer activity. *Mol. Pharm.* 13, 2423–2432.
- Syed Abdul Rahman, S.N., Abdul Wahab, N., Abd Malek, S.N., 2013. *In vitro* morphological assessment of apoptosis induced by antiproliferative constituents from the rhizomes of *Curcuma zedoaria*. *Evidence-Based Complementary Altern. Med.* 2013, 1–14.
- Taghdisi, S.M., Lavaee, P., Ramezani, M., Abnous, K., 2011. Reversible targeting and controlled release delivery of daunorubicin to cancer cells by aptamer-wrapped carbon nanotubes. *Eur. J. Pharm. Biopharm.* 77, 200–206.
- Trindade, G.S., Farias, S.L.A., Rumjanek, V.M., Capella, M.A.M., 2000. Methylene blue reverts multidrug resistance: sensitivity of multidrug resistant cells to this dye and its photodynamic action. *Cancer Lett.* 151, 161–167.
- Vasheghani Farahani, B., Rezaei Behbahani, G., Javadi, N., 2016. Functionalized multi walled carbon nanotubes as a carrier for doxorubicin: drug adsorption study and statistical optimization of drug loading by factorial design methodology. *J. Braz. Chem. Soc.* 27, 694–705.
- Vinothini, K., Rajendran, N., Ramu, A., Elumalai, N., Rajan, M., 2019. Folate receptor targeted delivery of paclitaxel to breast cancer cells via folic acid conjugated graphene oxide grafted methyl acrylate nanocarrier. *Biomed. Pharmacother.* 110, 906–917.
- Vinothini, K., Rajendran, N., Rajan, M., Ramu, A., Marraiki, N.M., Elgorban, A., 2020. A magnetic nanoparticles functionalized reduced graphene oxide-based drug carrier system for chemophotodynamic cancer therapy. *New J. Chem.* 44, 5265–5277.
- Vivek, R., Thangam, R., Nipunbabu, V., Ponraj, T., Kannan, S., 2014. Oxaliplatin-chitosan. nanoparticles induced intrinsic apoptotic signaling pathway: a “smart” drug delivery system to breastcancer cell therapy. *Int. J. Biol. Macromol.* 65, 289–297.
- Wei, C., Dong, X., Zhang, Y., Liang, J., Yang, A., Zhu, D., Liu, T., Kong, D., Lv, F., 2018. Simultaneous fluorescence imaging monitoring of the programmed release of dual drugs from a hydrogel-carbon nanotube delivery system. *Sens. Actuators, B* 273, 264–275.
- Wen, S., Liu, H., Cai, H., Shen, M., Shi, X., 2013. Targeted and pH-responsive delivery of doxorubicin to cancer cells using multifunctional dendrimer-modified multi-walled carbon nanotubes. *Adv. Healthcare Mater* 2, 1267–1276.
- Wu, H., Shi, H., Zhang, H., Wang, X., Yang, Y., Yu, C., Hao, C., Du, J., Hu, H., Yang, S., 2014. Prostate stem cell antigen antibody-conjugated multiwalled carbon nanotubes for targeted ultrasound imaging and drug delivery. *Biomaterials* 35, 5369–5380.
- Zhang, Y., Huang, F., Ren, C., Yang, L., Liu, J., Cheng, Z., Chu, L., Liu, J., 2017. Targeted chemo-photodynamic combination platform based on the DOX prodrug nanoparticles for enhanced cancer therapy. *ACS Appl. Mater. Interfaces* 9, 13016–13028.